G. Medic
e-mail: gmedic@stanford.edu

P. A. Durbin
e-mail: durbin@vk.stanford.edu

Mechanical Engineering Department,
Stanford University,
Stanford, CA 94305-3030

Toward Improved Film Cooling Prediction

Computations of flow and heat transfer for a film-cooled high pressure gas turbine rotor blade geometry are presented with an assessment of several turbulence models. Details of flow and temperature field predictions in the vicinity of cooling holes are examined. It is demonstrated that good predictions can be obtained when spurious turbulence energy production by the turbulence model is prevented. [DOI: 10.1115/1.1458021]

1 Introduction

In a companion paper [1], we demonstrated that the prediction of turbine blade heat transfer by two-equation turbulence closures could be greatly improved. In the absence of film cooling, the standard $k-\omega$ and two-layer $k-\epsilon$ models trend to overpredict the blade surface heat transfer coefficient, due mainly to the spurious production of turbulent energy under large rates of strain. This is a critical failing for turbomachinery applications—known, although not widely appreciated. It was demonstrated that this problem can be allayed by simple modifications of the native models. Either of the two cures proposed in [2] and [3] were found to give substantial improvement in predictions of heat transfer level. The term "limiter" can be used for this generic type of cure. In [1], the limiters improved heat transfer predictions by about 50 percent and reduced the excessive turbulent energy by a factor of about 30. It is known from theory and experiment that the level of k obtained with the limiters is far more plausible than without them.

The present paper extends the assessment to the problem of film cooling. Detailed computations of the flow through the film cooling hole and over the blade have previously met with limited success [4]. While the far-field full coverage film can be accurately computed, the near hole region is more difficult. Correct prediction of film-cooling heat transfer is directly related to the predicting how the jet mixes into the ambient cross-flow. Such predictions are strongly influenced by the choice of turbulence model.

Four configurations were studied in Camci and Arts [5–8], we will consider only two: suction side cooling and pressure side cooling, with different flow conditions. The overall flow is quite complex. It joins together the difficulties of computing the flow and associated heat transfer in a transonic cascade with the need for precise computations of the low speed flow in the cooling plenum and through the cooling holes. The velocity field in these holes is strongly non-uniform, with large secondary flow effects, see [4,9]. The cylindrical holes are conically shaped at the junction with the outer blade surface, adding the difficulty of accurately predicting diffuserlike geometries.

Computations of this test case have been presented in [10]. These authors used a simple algebraic turbulence model, without any detailed accounting for how the flow in the vicinity of the film cooling apparatus influences the turbulence. In the present paper, however, we find that predictions vary significantly with the different turbulence models, underlining the need to properly understand the coolant flow and its mixing with the mainstream.

Better understanding of the effects of hole geometry, and better predictions, especially of its influence on the local flow, could lead to the improvement of the hole geometry design process. More accurate computations might also make it possible to use predictive methods to optimize the positioning of cooling holes in the blade surface [11].

2 Film Cooling

The same experiment of [6], addressed in the companion article, is computed here for two cases with film cooling. The first is a double row of staggered axial cooling holes on the suction side of the blade; the other has a single row of cooling holes along the pressure side. Detailed experimental results for various configurations are published in Camci and Arts [5–8]. An outline of the blade, with the location of the cooling holes and plenum shown, is presented in Fig. 1.

On the suction side there are two rows (S) of staggered axial holes located at $s/c=0.206$, 0.237, with s measured from the leading edge, LM, and $c=80$ mm. They have diameter $d=0.8$ mm at their base, and are conically flared, with a 10 deg angle of expansion below the exit. The row and hole spacings are, respectively, 2.5 and 2.6 mm. These holes are inclined at 37 and 43 deg with respect to the local blade surface. A single row of conically shaped, axial holes ($d=0.8$ mm, 10 deg angle of expansion, $s/c=-0.315$) is located on the pressure surface (P). The hole spacing is 2.6 mm. These holes are inclined at 35 deg with respect to the local blade surface. More detailed description of the hole geometry can be found in Camci and Arts [5–7].

The flow through the cascade is under the same conditions as when there is no cooling present: $M_{in}=0.25$, $Re_{c,in}=8.5\cdot 10^5$, $Tu_{in}=5\%$, $T_{0\infty}=409.5$ K, inflow angle=30 deg, The exit Mach number is $M_{ex,is}=0.92$ and the wall temperature is $T_w=298$ K.

Several coolant inflow conditions were analyzed, both for the suction side and the pressure side cooling; notably, coolant temperatures T_c and blowing ratios $m=U_c\rho_c/(U_\infty\rho_\infty)$ were varied. Here, $U_c\rho_c$ is obtained from the mass flux and hole area, and $U_\infty\rho_\infty$ is found from local surface pressure, inlet total pressure and isentropic relations.

The experimental data are presented in the form of spanwise-averaged heat transfer coefficient h_t for a given wall temperature T_w (and not in the form of adiabatic effectiveness). Thus, we compare the heat transfer coefficient h_t with the computational predictions obtained with different turbulence models.

2.1 Numerical Procedure. For the process of numerical solution of flow equations, the turbulence models (modifications of two-layer $k-\epsilon$, standard and modified $k-\omega$ and v^2-f) were implemented into an implicit finite volume solver based on a variant of the well known SIMPLE method (see [12]), with the turbulence model equations decoupled and solved sequentially, for details see also [1].

Generation of a computational mesh for this flow presents a major challenge. We have opted for a multi-block, structured mesh having nonmatching (or non-conforming) interfaces. This

Contributed by the International Gas Turbine Institute for publication in the JOURNAL OF TURBOMACHINERY. Manuscript received by the IGTI, March 20, 2001; revised manuscript received Octoer 15, 2001. Associate Editor: R. Bunker.

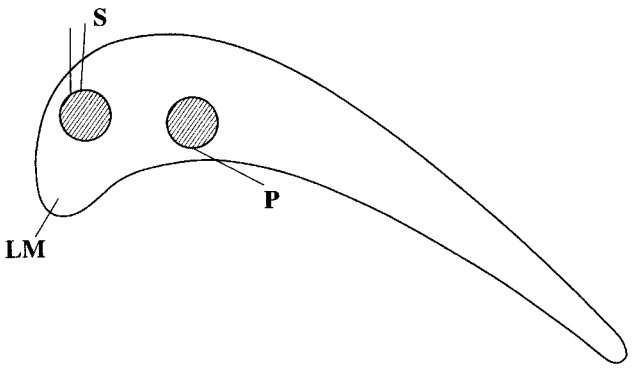

Fig. 1 Geometry of cooling holes

gives significant flexibility in generating generic mesh-blocks for different film cooling configurations—suction side cooling holes, pressure side holes, leading edge cooling, etc.

There are four non-matching mesh blocks: a plenum mesh; a mesh in the conical tubes; a portion of very fine outer O-mesh just above the cooling holes; and the rest of the outer O-mesh. Figures 2 and 3 are details of the grid near the cooling holes. It shows the higher resolution needed to capture the jet.

This topology, together with the mesh independence testing, lead to the final computational mesh of 750,000 vertices, with sufficiently fine resolution in the region of the holes.

Another matter of concern was specification of inflow boundary conditions for the coolant. The coolant plenum was included in the analysis, since the flow at the entrance to the cooling holes is far from being uniform and the length of the cooling tubes $L/D = 5-6$ implies that at the exit of the cooling tube the flow is not yet completely developed, see also [4] and [13]. Details of the flow field in the vicinity of the plenum-tube junction for the suction side holes are presented in Fig. 4. There is a low-momentum region at the inner wall of the tubes, induced by the turning of the flow into the cooling tubes. This leads to generation of high levels of turbulent kinetic energy at the boundary of that low momentum region inside the tubes. Such an effect can be seen in the v^2-f computations presented in Fig. 5.

To match experimental blowing ratios, it was necessary to iteratively adjust the plenum pressure. This is a computationally expensive procedure, but a good match to experimental conditions was obtained.

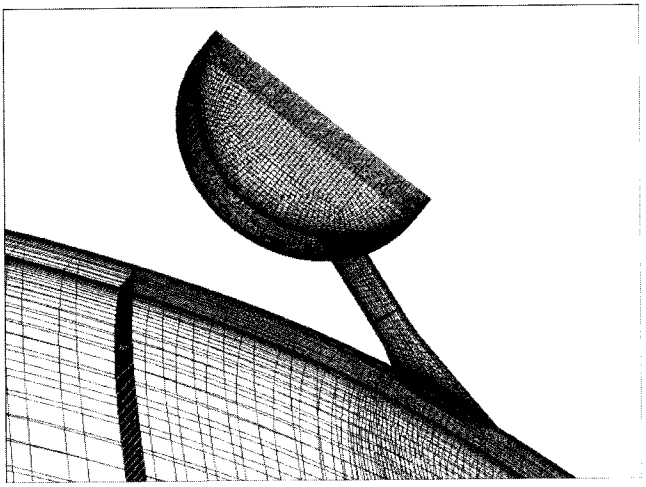

Fig. 3 Detail of the computational mesh, pressure side cooling holes

The appropriate boundary conditions for turbulence in the plenum are uncertain. To see whether this had any bearing on our results we have tested several levels of turbulence intensity, up to 20 percent. No significant effect on the film cooling predictions was observed since the flow in the plenum has very low velocity compared to the flow in the tubes, and the same goes for the value of turbulent kinetic energy when compared to the level of turbulent kinetic energy produced at the entrance of cooling tubes.

There was also some concern over the question of the appropriate inflow temperature to the plenum. For coolant temperatures, T_c, lower than the wall temperature, T_w, it was not clear whether heat transfer occurs in the plenum via conduction through the walls. To eliminate this uncertainty, we chose to consider the isothermal case, $T_c = T_w$, exclusively. A few calculations were done with $T_c = 0.7T_w$: they showed lower h_t near the exit of the cooling holes than the isothermal case. Experiments showed a smaller level of difference between the cold jet and isothermal cases, but the exit region is where preheating effects would be most significant.

In the results presented in [1] it was seen that the standard $k-\epsilon$ and $k-\omega$ models grossly overpredict the heat transfer coefficient h_t in the absence of film cooling. When either of the two

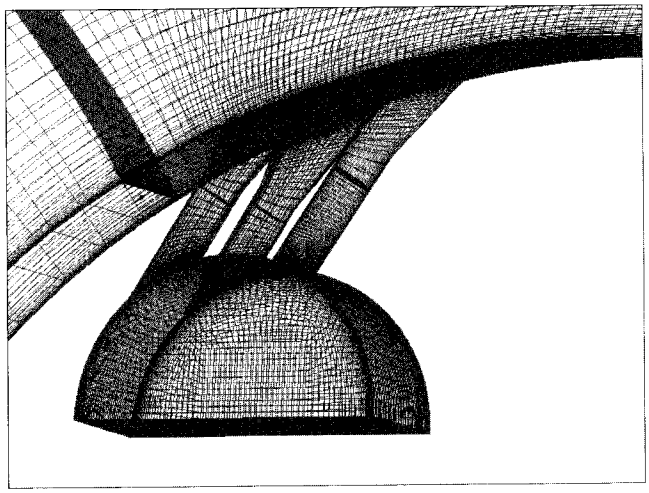

Fig. 2 Detail of the computational mesh, suction side cooling holes

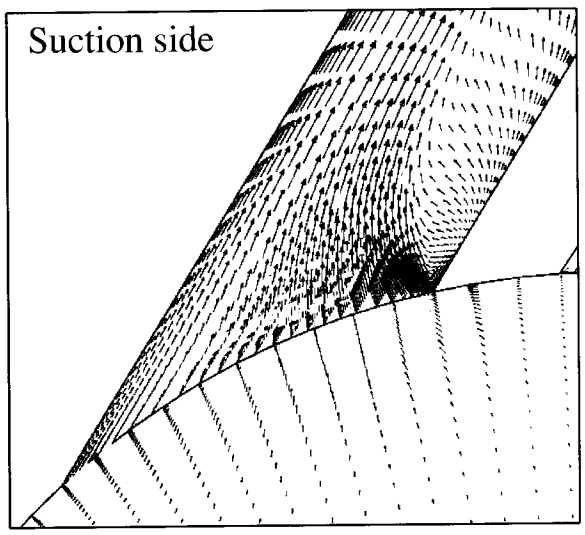

Fig. 4 Detail of velocity vectors in the plenum-tube junction region, computations with v^2-f model

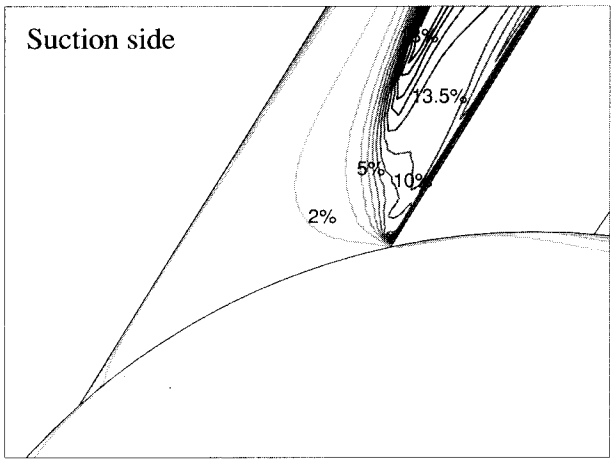

Fig. 5 Detail of turbulent intensity contours in the plenum-tube junction region, computations with v^2-f model

limiters were invoked, correct levels of heat transfer coefficient were predicted over most of the blade (with the primary exception in a zone on the suction side, near the leading edge).

This tendency was confirmed in the present cases with film cooling; the high values of turbulent viscosity in the passage predicted by the standard $k-\epsilon$ model led to overprediction of heat transfer coefficient downstream of cooling holes. For that reason, the majority of our comparisons of numerical solutions to experimental data on heat transfer will be for the $k-\epsilon$ model with a bound on turbulent time-scale and for the v^2-f model.

2.2 Suction Side Film Cooling. The coolant inflow conditions of Camci and Arts [5–7] for the suction side were blowing ratios in the range $m=0.45-1.0$, and temperatures in the range $T_c/T_w=0.6-1.0$. For the reason given in the foregoing, we will consider only the isothermal case, $T_c=T_w$. Since the numerical results for lower blowing ratios ($m=0.45$ and 0.60) tend to agree better with the experimental data, we will put more attention to detailed analysis of the flow field for the high blowing ratio, $m=1.0$; See Fig. 6.

As seen in Figs. 7 and 8, for lower blowing ratios the spanwise-averaged heat transfer coefficient h_t is predicted reasonably well, both with the $k-\epsilon$ model, invoking the bound on the turbulent time scale T, and with the v^2-f model. Near the hole the $k-\epsilon$ solution is in good agreement with data, while the v^2-f prediction is low.

However, for the high blowing ratio, $m=1.0$, Fig. 9 evidences are more significant discrepancies with the experimental data, especially in the vicinity of the film cooling holes. This figure presents results with four models that were assessed for the flow without cooling; the standard, two-layer $k-\epsilon$, the [2] modification to production, the time-scale limit [3], and v^2-f. Kato-Launder predictions of h_t are a bit higher than obtained with the time scale bound, and a bit higher than the data in the downstream region. The native $k-\epsilon$ model grossly overpredicts heat transfer

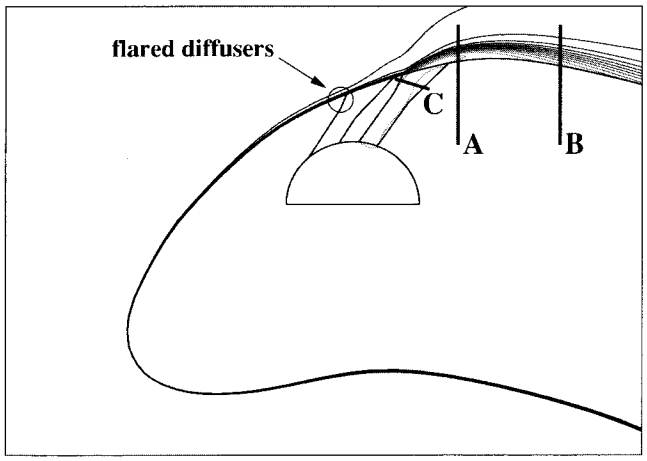

Fig. 6 Temperature and location of characteristic cross sections, $m=1.0$

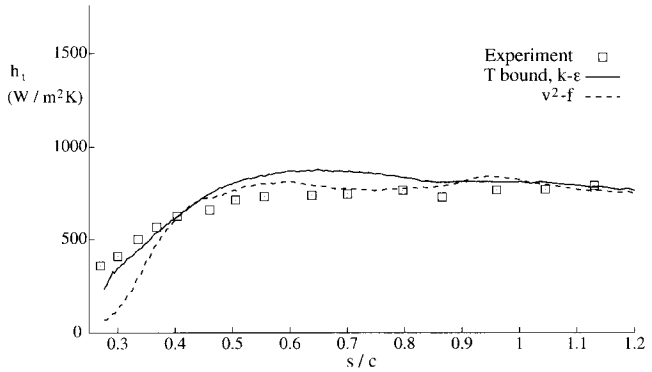

Fig. 7 Heat transfer coefficient, h_t (W/m²K), suction side cooling, $m=0.45$

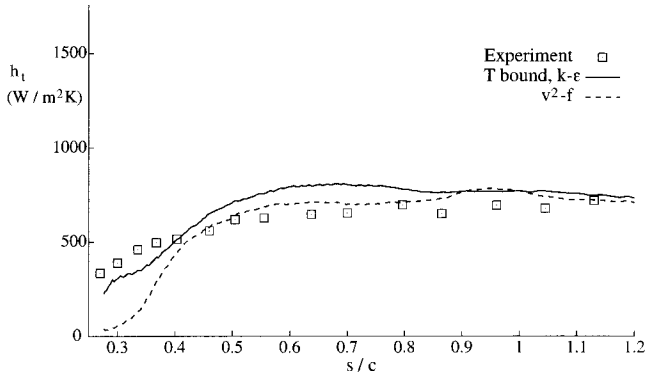

Fig. 8 Heat transfer coefficient, h_t (W/m²K), suction side cooling, $m=0.6$

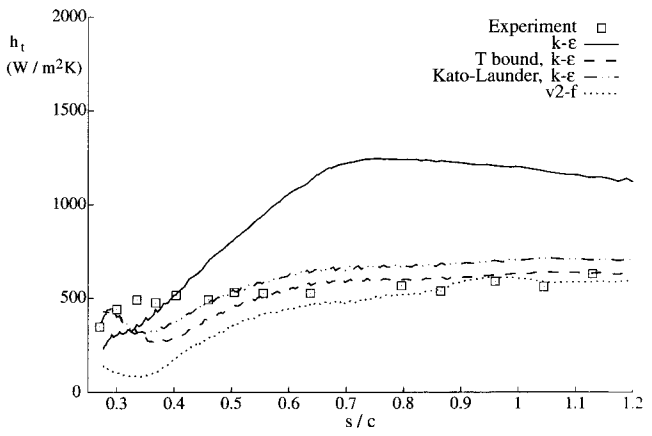

Fig. 9 Heat transfer coefficient, h_t (W/m²K), suction side cooling, $m=1.0$

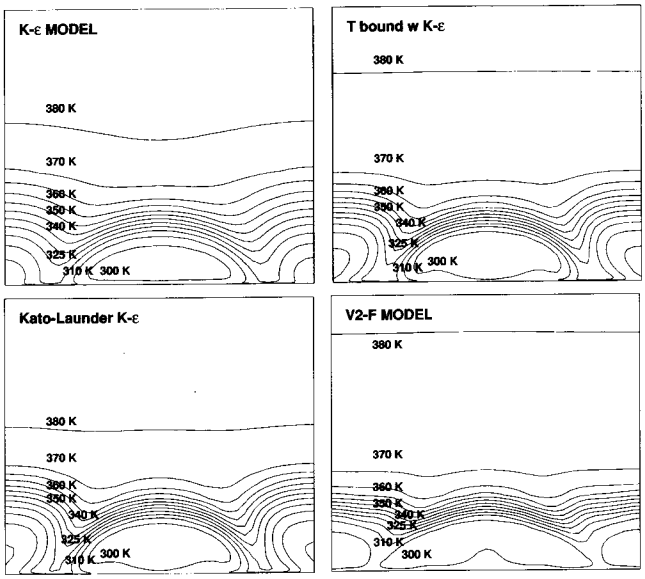

Fig. 10 Temperature contours computed with different turbulence models, cross section A, suction side cooling, high blowing ratio m=1.0

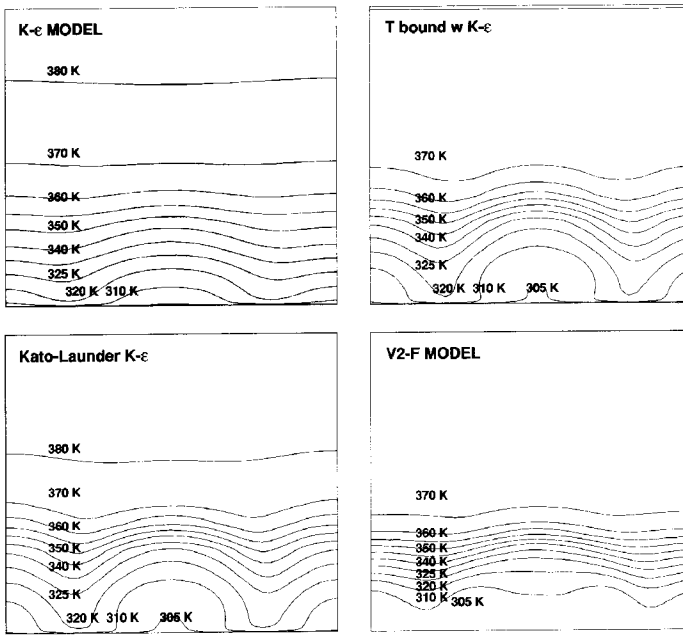

Fig. 11 Temperature contours computed with different models, cross section B, suction side cooling, high blowing ratio m=1.0

in the downstream region. This is due to excessive production of turbulence by the straining flow in the center of the passage. The excessive energy penetrates the boundary layer, leading to the increase of wall heat transfer (as in the case without cooling); the predictions h_t become completely erroneous.

Finally, the v^2-f model tends to predict the correct level of heat transfer coefficient downstream of the cooling holes, but not in the vicinity of the holes. There the level of cooling is overpredicted, resulting in lower values of h_t.

In order to better understand the computational predictions in the vicinity of the cooling holes, some relevant quantities were plotted in cross flow planes. Attention is focused on this blowing ratio of $m=1.0$. The following discusses fields of temperature, turbulence intensity, crossflow velocity and velocity magnitude, obtained with the various turbulence models. The locations of these characteristic cross-sections are shown in Fig. 6: axial sections (x=const) A and B are located at $s/c=0.28$ and 0.35, respectively; section C is located at 3/4 of the height of the second cooling tube.

Temperature contours in cross sections A and B are presented in Figs. 10 and 11. They reveal that the v^2-f model predicts the greatest spanwise spreading of the region of cold temperature, in the core of the cooling jet. All three $k-\epsilon$ results (standard, T bound, Kato-Launder) show less lateral spreading near the hole. The lateral spreading is due to a pair of counter-rotating, streamwise vortices that form on either side of the hole. Stronger spreading causes lower heat transfer because the jet shields the surface from the hot ambient.

Further downstream, in cross section (B), high turbulent viscosity is predicted by the standard $k-\epsilon$ model, leading to more diffusion. This causes high temperatures to penetrate from the free-stream significantly closer to the blade surface than with other models.

Turbulence intensity contours in the same cross sections (Figs. 12 and 13) seem to be consistent with what was observed in the case without cooling [1]—the native $k-\epsilon$ model, with no limiters, strongly overpredicts turbulence levels.

Examining the velocity magnitude contours inside the second row of cooling holes (Fig. 14, which is a plane normal to the axis of the hole), we can see that the kidney-shaped core of the jet predicted with the v^2-f model seems to be slightly larger than with the other models. This larger high velocity region is probably a result of a weaker recirculation near the walls of this diffuser part of the tube.

It seems that differences in the magnitude of crossflow, as well in the high-velocity core of the jet, alter the extent of jet penetration into the mainstream and of the lateral spreading of cool fluid. These differences originate *inside* the hole. Their effect on turbulence production and the level of turbulent viscosity in the near wall region is equally important. The v^2-f model leads to a stronger interaction between the two rows of jets, and therefore to more spreading of coolant across the blade surface in the spanwise direction. $k-\epsilon$ predicts a higher near-wall eddy viscosity.

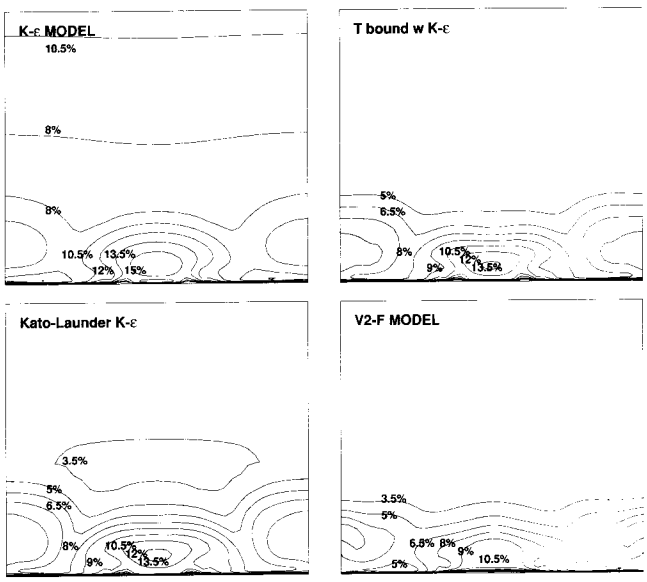

Fig. 12 Turbulence intensity computed with various models, cross section A, suction side cooling, high blowing ratio m=1.0

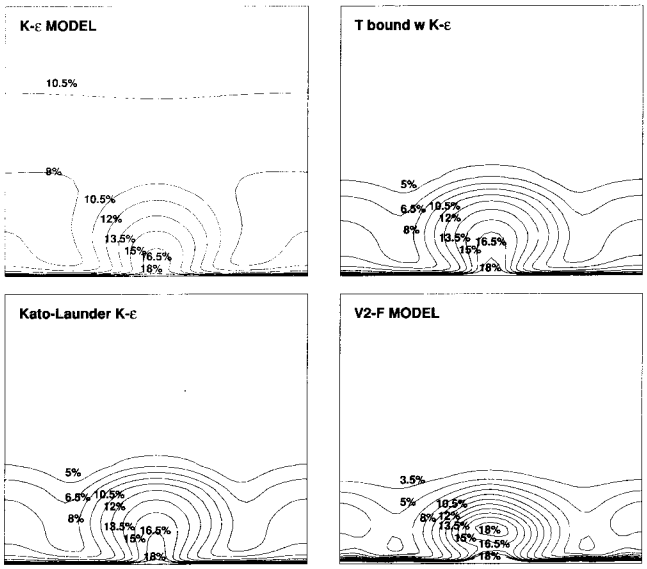

Fig. 13 Turbulence intensity computed with various models, cross section B, suction side cooling, high blowing ratio m=1.0

2.3 Pressure Side Film Cooling. The inflow boundary conditions for the coolant for the pressure side experiments of Camci [5] were blowing ratios in the range m=1.75–4.25 (see Fig. 15), and temperatures in the range T_c/T_w=0.6–1.0. As before, only the isothermal case $T_c=T_w$ will be considered; the experimental blowing ratios were 1.74, 3.28, and 4.23.

Similarly to the suction side cooling, lower blowing ratio cases are easier to compute. As can be seen from h_t predictions with m=1.75 in Fig. 16, solutions to the $k-\epsilon$ model with the bound on T invoked, agree reasonably well with the experimental measurements.

However, increasing the blowing ratio leads to the situation where the jet actually penetrates into the mainstream; see also [5]. As a consequence, a region of increased heat transfer occurs just downstream of cooling holes ($s/c\approx-0.35$ in Fig. 18)—near the holes without cooling h_t was about 20 percent lower. This phenomenon is difficult to compute accurately. The spanwise averaged heat transfer coefficient for m=3.3 and 4.25 is provided in Figs. 17 and 18, respectively.

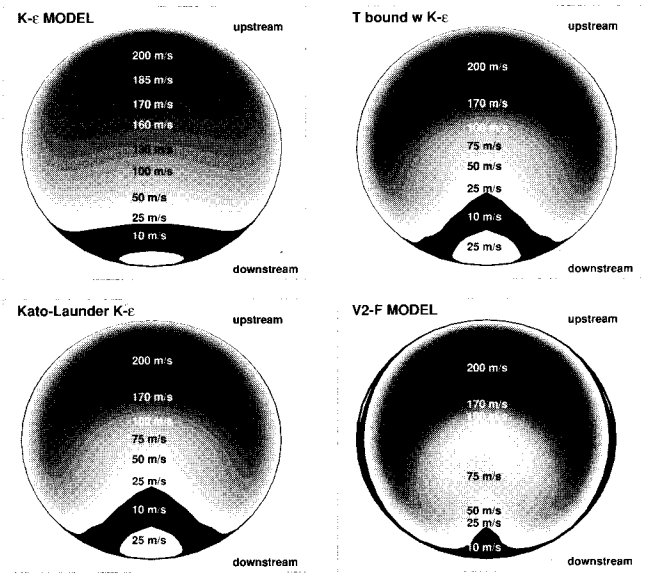

Fig. 14 Velocity magnitude with different models, cross section C, suction side cooling, high blowing ratio m=1.0 (cascade inflow U_{inflow}=100 m/s)

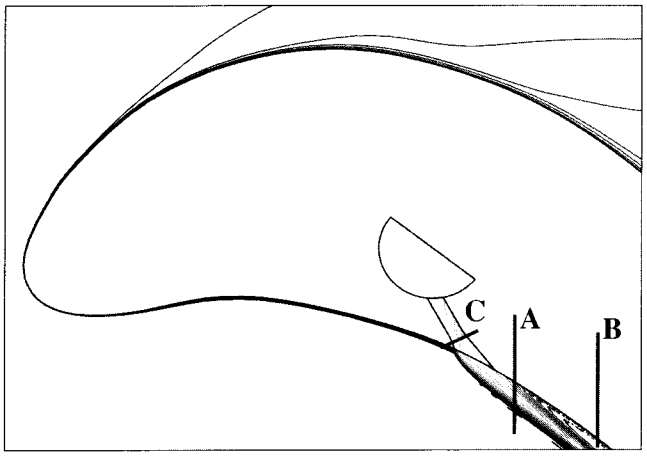

Fig. 15 Temperature and location of characteristic cross sections, m=4.25

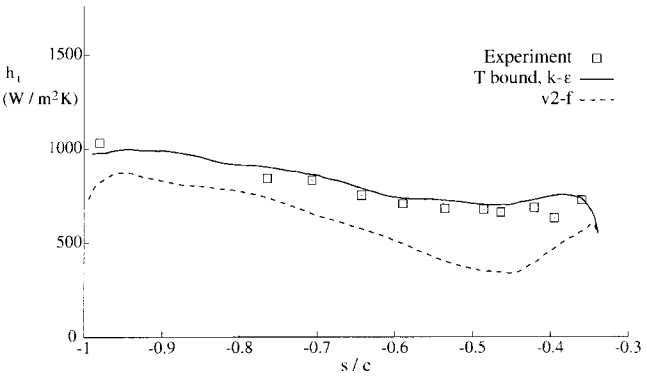

Fig. 16 Heat transfer coefficient, h_t (W/m²K), pressure side cooling, m=1.75

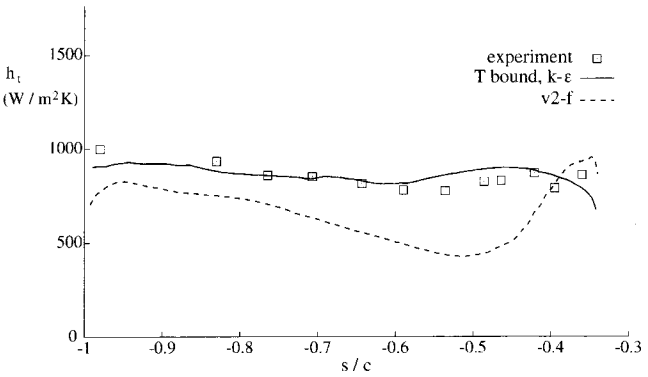

Fig. 17 Heat transfer coefficient, h_t (W/m²K), pressure side cooling, m=3.3

The predictions vary significantly in the vicinity of the cooling holes. The standard $k-\epsilon$ model gives predictions that are similar to the case of suction side cooling: further downstream the over estimation of turbulence level in the passage leads to an overprediction of wall heat transfer. (Note that the downstream direction in Figs. 16–18 is to the left, $s/c\rightarrow-1$.)

The v^2-f model does not recover to the right level. This is consistent with the results without film cooling in [1], where v^2

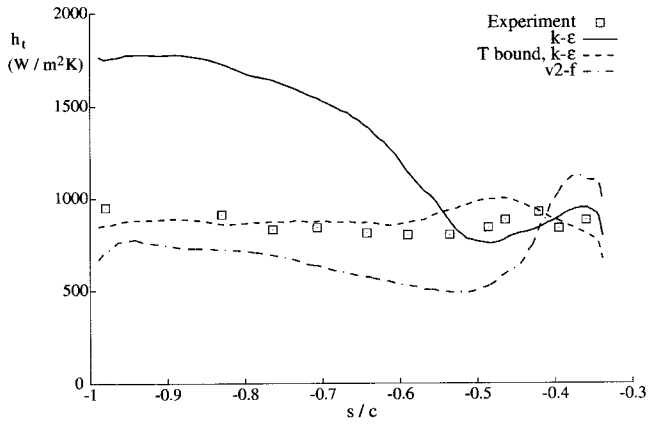

Fig. 18 Heat transfer coefficient, h_t (W/m²K), pressure side cooling, m=4.25

$-f$ already tended to underpredict the heat transfer towards the rear of the pressure side. The main discrepancy is due to the baseline h_t, not to the film cooling, *per se*. On the other hand, the predictions with the $k-\epsilon$ model with the time-scale bound in place, seem to be in even better agreement with experiments than for suction side cooling. It is quite remarkable that this simple modification to the time-scale can improve predictions so substantially.

As for the suction side cooling, we will investigate the flow fields more closely for the high blowing ratio, m=4.25. Contour plots are provided at a few characteristic cross-sections, presented in Fig. 15. Axial sections (x=const) A and B are located at $s/c = -0.35$ and -0.45, respectively, section C is at 3/4 of the height of the cooling tube.

Comparing the computed temperature contours in cross-sections A and B (Figs. 19 and 20), one observes similar tendencies as for the suction side cooling. The core of the jet predicted by v^2-f model spreads more in the spanwise direction than with the other models. Figure 19 shows a temperature minimum well above the boundary layer, with higher temperatures penetrating under the jet; this is by contrast to Fig. 10, where the temperature

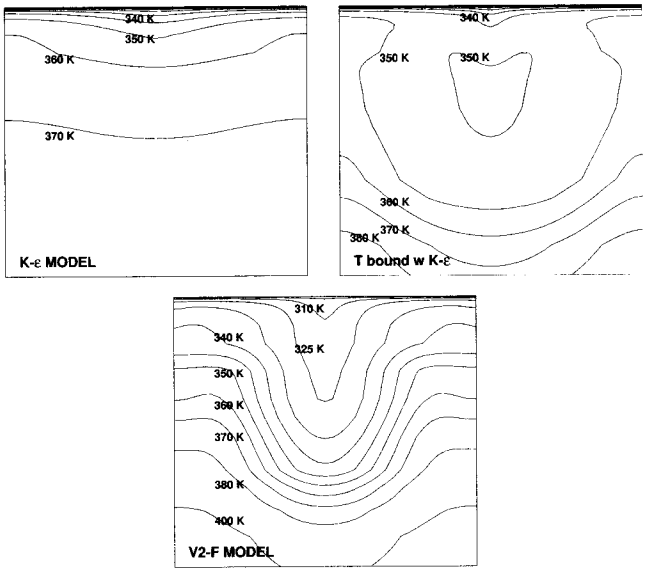

Fig. 20 Temperature contours computed with different models, cross section B, pressure side cooling, high blowing ratio m=4.25 (blade surface at the top)

minimum is adjacent to the surface. Thus, the jet is seen to have lifted from the wall at the blowing ratio m=4.25. Downstream, at section B, the elevated cold spot has largely dispersed, although it is still detectable in the modified $k-\epsilon$ solution (Fig. 20). Although the link between surface heat flux and the jet trajectory is somewhat circumstantial, it is generally believed that correct h_t predictions depend strongly on correct jet lift-off.

Finally, the velocity magnitude contours inside the tube, at cross section C, are presented in Fig. 21. Similar effects to the suction side case can be seen: slightly high velocity in the core of the jet predicted with the v^2-f model, and a slightly smaller low-speed region on the downstream side.

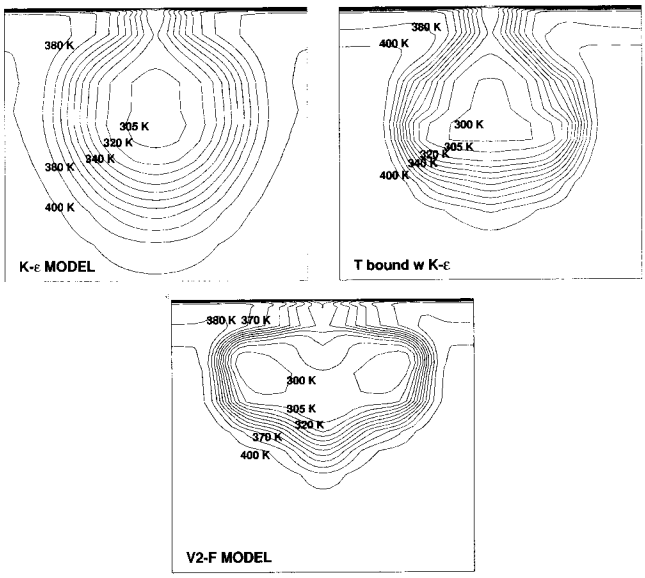

Fig. 19 Temperature contours computed with various turbulence models, cross section A, pressure side cooling, high blowing ratio m=4.25 (blade surface at the top)

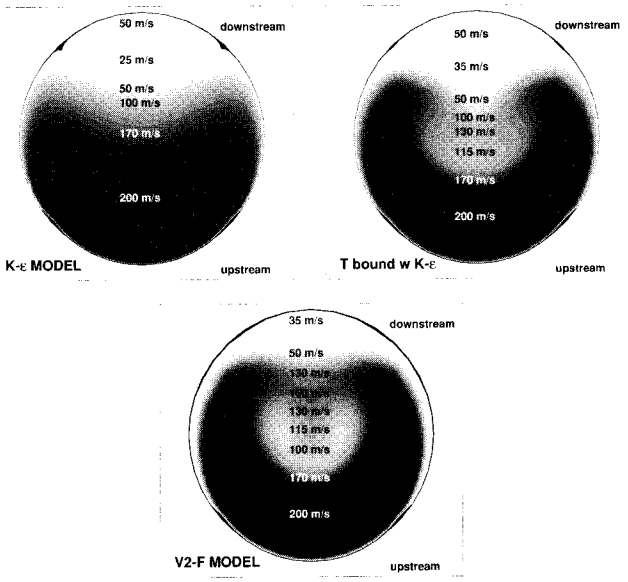

Fig. 21 Velocity magnitude with different models, cross section C, pressure side cooling, high blowing ratio m=4.25 (cascade inflow U_{inflow}=100 m/s)

3 Conclusions

In [1] and here, we have conducted detailed analysis of an experimentally documented test case. Turbulence models meant for practical, engineering flow computation have been used. Results were presented for the flow in the absence of, and with film cooling.

The most practically significant result of this study is that the native $k-\epsilon$ or $k-\omega$ models can give wildly unreasonable predictions of heat transfer in turbine passages. This fault is readily cured by invoking a bound on turbulent time scale. This *does not mean that the solution is clipped*; rather where a time-scale is needed, such as in the formula $\nu_t = C_\mu kT$, the bounded value is used. For instance, the $k-\omega$ eddy viscosity becomes

$$\nu_t = k \times \min\left[\frac{1}{\omega}, \frac{\alpha}{\sqrt{6}|S|}\right]$$

rather than $\nu_t = k/\omega$.

Numerical results for film cooling show that the $k-\epsilon$ model using the bound for turbulent time-scale T and the v^2-f model give satisfactory predictions of the overall heat transfer coefficient levels, except for high blowing ratios. On the suction side, they tend to overpredict the level of cooling in the vicinity of the film holes, that being true especially for v^2-f computations. On the pressure side the cooling jet penetrates into the mainstream, and it appears that the v^2-f model predicts stronger jet lateral spreading than the other models. This seems to originate inside the diffusing section of the cooling hole.

This analysis of film cooling represents a step in the direction of proper understanding of the effects of hole geometry and especially its influence on the local flow field, as well as better understanding of computational predictions using various turbulence models.

Acknowledgments

This work was sponsored by General Electric Aircraft Engines.

Nomenclature

- M = Mach no.
- $\mathrm{Re}_{c\text{-}in}$ = inflow Reynolds no. (based on chord length c)
- T_o = total temperature
- T_w = wall temperature
- T_c = coolant inflow temperature
- Tu = turbulence intensity $= \sqrt{2/3\,k}/|U|$
- c = blade chord
- h_t = heat transfer coefficient $= \dot{q}_w/(T_{o\infty} - T_w)$
- k = turbulent kinetic energy (per unit mass)
- m = blowing ratio $= U_c\rho_c/(U_\infty\rho_\infty)$, based on local free stream values
- $\dot{q}_w$ = wall heat flux rate
- s = curvilinear coordinate
- ϵ = rate of turbulent energy dissipation

Subscripts

- ∞ = free stream
- c = coolant inflow
- in = inflow
- ex = exit
- w = wall
- o = total conditions
- is = isentropic conditions

References

[1] Medic, G., and Durbin, P. A., 2002, "Toward Improved Prediction of Heat Transfer on Turbine Blades," ASME J. Turbomach., **124**, pp. 187–192.

[2] Launder, B. E., and Kato, M., 1993, Modelling Flow-Induced Oscillations in Turbulent Flow Around a Square Cylinder," ASME FED **157**, pp. 189–199.

[3] Durbin, P. A., 1996, "On the $k-\epsilon$ Stagnation Point Anomaly," Int. J. Heat Fluid Flow, **17**, pp. 89–90.

[4] Leylek, J. H., and Zerkle, R. D., 1994, "Discrete-Jet Film Cooling: A Comparison of Computational Results with Experiments," ASME J. Turbomach., **116**, pp. 358–368.

[5] Camci, C., 1985, *Theoretical and Experimental Investigation of Film Cooling Heat Transfer on a Gas Turbine Blade*, Ph.D. thesis, Von Karman Institute for Fluid Dynamics and University of Leuven, Belgium.

[6] Camci, C., and Arts, T., 1985a, "Short Duration Measurements and Numerical Simulation of Heat Transfer Along the Suction Side of a Film-Cooled Gas Turbine Blade," ASME J. Eng. Power, **107**, pp. 991–997.

[7] Camci, C., and Arts, T., 1985b, "Experimental Heat Transfer Investigation Around the Film-Cooled Leading Edge of a High-Pressure Gas Turbine Rotor Blade," ASME J. Eng. Power, **107**, pp. 1016–1021.

[8] Camci, C., and Arts, T., 1990, "An Experimental Convective Heat Transfer Investigation Around a Film-Cooled Gas Turbine Blade," ASME J. Turbomach., **112**, pp. 497–503.

[9] Walters, D. K., and Leylek, J. H., 2000, "A Detailed Analysis of Film Cooling Physics: Part I—Streamwise Injection With Cylindrical Holes," ASME J. Turbomach., **122**, pp. 102–112.

[10] Garg, V. K., and Gaugler, R. E., 1997, "Effect of Coolant Temperature and Mass Flow on Film Cooling of Turbine Blades," Int. J. Heat Mass Transf., **40**, 435–445.

[11] Friedrics, S., Hodson, H. P., and Dawes, W. N., 1999, "The Design of an Improved Endwall Film-Cooling Configuration," ASME J. Turbomach., **121**, pp. 772–780.

[12] STAR-CD Version 3.10—Methodology, 1999, Computational Dynamics Limited.

[13] Hale, C. A., Plesniak, M. W., and Ramadhyani, S., 2000, "Film Cooling Effectiveness for Short Film Cooling Holes Fed by a Narrow Plenum," ASME J. Turbomach., **122**, pp. 553–557.